Agricultural and Forest Meteorology 262 (2018) 192–205

Contents lists available at ScienceDirect

Agricultural and Forest Meteorology

journal homepage: www.elsevier.com/locate/agrformet

Decomposing sources of uncertainty in climate change projections of boreal forest primary production

Tuomo Kalliokoski[a,b,*], Annikki Mäkelä[b], Stefan Fronzek[c], Francesco Minunno[b], Mikko Peltoniemi[d]

[a] University of Helsinki, Department of Physics, P.O. Box 64, FI-00014, Finland
[b] University of Helsinki, Department of Forest Sciences, P.O. Box 27, FI-00014, Finland
[c] Finnish Environment Institute, P.O. Box 140, Helsinki FI-00260, Finland
[d] Natural Resources Institute Finland, Latokartanonkaari 9, Helsinki FI-00790, Finland

ARTICLE INFO

Keywords:
Photosynthetic efficiency
Ecosystem response
Environmental change
Ecophysiology

ABSTRACT

We are bound to large uncertainties when considering impacts of climate change on forest productivity. Studies formally acknowledging and determining the relative importance of different sources of this uncertainty are still scarce, although the choice of the climate scenario, and e.g. the assumption of the CO_2 effects on tree water use can easily result in contradicting conclusions of future forest productivity. In a large scale, forest productivity is primarily driven by two large fluxes, gross primary production (GPP), which is the source for all carbon in forest ecosystems, and heterotrophic respiration. Here we show how uncertainty of GPP projections of Finnish boreal forests divides between input, mechanistic and parametric uncertainty. We used the simple semi-empirical stand GPP and water balance model PRELES with an ensemble of downscaled global circulation model (GCM) projections for the 21st century under different emissions and forcing scenarios (both RCP and SRES). We also evaluated the sensitivity of assumptions of the relationships between atmospheric CO_2 concentration (C_a), photosynthesis and water use of trees. Even mean changes in climate projections of different meteorological variables for Finland were so high that it is likely that the primary productivity of forests will increase by the end of the century. The scale of productivity change largely depends on the long-term C_a fertilization effect on GPP and transpiration. However, GCM variability was the major source of uncertainty until 2060, after which emission scenario/pathway became the dominant factor. Large uncertainties with a wide range of projections can make it more difficult to draw ecologically meaningful conclusions especially on the local to regional scales, yet a thorough assessment of uncertainties is important for drawing robust conclusions.

1. Introduction

Understanding the development of forest productivity in a changing environment is pivotal for making decisions about forest use in the future. Such understanding is also needed for improving the climate projections themselves, as a large proportion of uncertainty of global warming projections arises from uncertainties in modelling terrestrial phenomena and their biophysical interactions with climate (Bonan, 2008). Boreal forests play a large role in determining the global mean temperature (Snyder et al., 2004; Snyder and Liess, 2014), and are generally assumed to provide climate mitigation potential due to projected increased growth and carbon sequestration under climate change (IPCC et al., 2013), although the biophysical effects like albedo or biogenic volatile organic compounds (BVOCs) may change the net impact (Bright et al., 2014; Unger, 2014). Opposing trends may also emerge as a result of increased utilization of forests for the production of bioenergy and new bio-based products (Ollikainen, 2014). For example in Finland, recent impact studies suggest an increase of 5–27% in productivity of Norway spruce until end of this century (Ge et al., 2013 using SRES A2 scenarios, Reyer et al., 2014 using SRES A1B). However, all impact studies include a lot of uncertainty related to model structure, parameter values, and climate input data, which has not been systematically analysed in boreal forest studies. The lack of including these in the assessment of uncertainty may lead to suboptimal decision-making from the climate change mitigation perspective.

In a large scale comparison, forest productivity is primarily driven by two large fluxes, gross primary production (GPP), which is the source carbon for all carbon in forest ecosystems (Ma et al., 2015), and

* Corresponding author at: University of Helsinki, Department of Physics, P.O. Box 64, FI-00014, Finland.
E-mail address: tuomo.kalliokoski@helsinki.fi (T. Kalliokoski).

https://doi.org/10.1016/j.agrformet.2018.06.030
Received 18 November 2017; Received in revised form 27 June 2018; Accepted 30 June 2018
Available online 20 July 2018
0168-1923/

heterotrophic respiration. Correlations can therefore be found along environmental gradients between GPP and Net Primary Production (NPP; Waring et al., 1998; Mäkelä and Valentine, 2001; Dewar et al., 1998), litter fall (Reich et al., 2014; Mäkelä et al., 2016) and carbon accumulation in the soil (Liski et al., 2006). Recent decades have witnessed a profound development of models of canopy GPP, thanks to improved measurements and data from eddy flux networks where carbon and water fluxes are measured globally over different land cover types (e.g.FLUXNET, https://fluxnet.fluxdata.org). This has considerably improved the reliability of GPP predictions under current climate as a function of weather and canopy type (e.g. Novick et al., 2015; Wagle et al., 2016), sometimes also with generic models that do not require site-specific parameterisation (Minunno et al., 2016). Model-data assimilation techniques such as Bayesian model calibration also provide an improved understanding of the uncertainties of model parameters and how they propagate to model predictions (van Oijen et al., 2013; Minunno et al., 2016). The significance of GPP for ecosystem functioning, combined with a sound understanding of the process under the current climate, makes GPP simulatons an appropriate example case for exploring the types of uncertainty we are bound to face in future impact projections in a changing climate.

Uncertainties in model predictions generally originate in input uncertainty and model uncertainty (cf. Uusitalo et al., 2015). In climate change projections, input uncertainty includes uncertainties about climate scenario and climate development under a given scenario, demonstrated in the differences between climate models. In addition, there is uncertainty caused by natural variability of weather. Model uncertainty consists of parametric and structural uncertainty.

An important structural uncertainty for GPP prediction arises from the fact that the interactions of elevated atmospheric CO_2 concentrations (C_a) with changing climate are still poorly understood due to the limited possibilities of theory and model testing in experimental and natural conditions. In modelling studies, even more than half of the projected forest productivity has been attributed to increasing C_a (Bergh et al., 2003; Reyer et al., 2014) while without C_a fertilization, simulated forest productivity has even been predicted to decrease under climate change (Ollinger et al., 2007; Medlyn et al., 2011). While it is generally accepted that elevated C_a increases the water use efficiency of plants (WUE), the extent and mechanisms of this effect are not clear. Analyses of eddy-covariance measurements of the past 15 years have suggested even larger improvements of WUE than predicted by prevailing theories (Keenan et al., 2013). While studies where C_a concentration has been increased in the field (Free-Air Carbon dioxide Enrichment, FACE) have shown that trees increase their photosynthetic rates and still reduce stomatal conductance (Ainsworth and Rogers, 2007), the long-term ecosystem level responses depend on ecosystem type. Direct responses of trees to elevated C_a may become diluted in time, as physiological processes and tree structure acclimate to new conditions (Norby and Zak, 2011). For example, some studies have predicted spruce decline in southern Finland (Kellomäki et al., 2008; Ge et al., 2013), but the result strongly depends on the assumptions of C_a effects on transpiration.

The impact uncertainty arising from uncertainties in global circulation model (GCM) outputs has largely been ignored in (forest productivity in the boreal zone, although it has been investigated in the context of e.g. disturbances (Lehtonen et al., 2016). It is well known that projections of climate models can differ more between each other than projections of one specific climate model between emission scenarios (e.g. van Vuuren et al., 2011; Ahlström et al., 2012; Nishina et al., 2015). In the case of Finland, only few GCMs project mean annual temperature changes below 2 °C between the periods 1971–2000 and 2070–2099, even when assuming a low emission scenario (SRESB1) or a low emission Representative Concentration Pathway (RCP2.6) (Fig. 1). The respective changes in the high-end scenarios reach up to 10 °C (under RCP8.5 forcing, see Jylhä et al., 2009; Rötter et al., 2013; Ruosteenoja et al., 2016). The change in winter temperatures in January may be twice as large as the change in summer temperatures in July. Uncertainties in precipitation changes are much larger, but increases are expected especially in winter (Rötter et al., 2013; Jylhä et al., 2009). The frequent approach of using the ensemble mean of climate model variables as input to ecosystem models (e.g. Peltola et al., 2010; Veijalainen et al., 2010; Sievänen et al., 2014) is questionable since it may violate the coherence between different climate variables.

The objective of this study was to predict gross primary production (P) and plant-water relations of boreal forests in Finland using climate scenarios for the 21st century from ensembles of GCMs with different forcings (both RCP and SRES). By showing both scenario families we acknowledge the fact that SRES scenarios are still used in impact studies, and even more so in policy analyses. Comparing the two sets of scenarios will help us put the SRES scenario results in perspective with those obtained from the RCP scenarios. We calculated P using a simple ecosystem flux model, PRELES, (Peltoniemi et al., 2015) with a generic boreal parameterisation (Minunno et al., 2016). We then quantified and compared the different sources of uncertainty, including the parametric uncertainty obtained from data-model assimilation, the structural uncertainty of C_a fertilization and water use effects, and input uncertainties originating in stochastic variability of weather and uncertainty created by the choice of climate model and forcing scenario. Using our study on GPP as an example, we discuss the implications more broadly in the framework of ecological impact model applications that are subject to large uncertainties.

2. Materials & methods

2.1. The PRELES model

The PRELES model (Peltoniemi et al., 2015) describes P and water exchange (evapotranspiration, E) of forest canopies on the basis of light use efficiency (LUE), expressed as a multiplicative model of potential LUE and environmental modifiers f_i ($0 < f_i < 1$). It inherits its photosynthesis part from Mäkelä et al. (2008a,b) while a simple description of daily soil water balance was made in Peltoniemi et al. (2015). The model has been calibrated to eddy-covariance derived data on P, E, and measurements of soil water in Scots pine stands (Peltoniemi et al., 2015), and a generic, species-independent parameterisation for boreal stands has been prepared (Minunno et al., 2016). While the existing model parameterisation has been carried out in current climate under constant C_a, here we extend the model to be applicable to future environment by incorporating an additional C_a modifier. Here we first outline the structure of the model, then introduce our treatment of the sources of mechanistic and input uncertainty. The details of PRELES are presented in Peltoniemi et al. (2015).

The photosynthetic production P (gC m^{-2} day^{-1}) is predicted in PRELES as:

$$P = f_{aPPFD}\ P_0 \equiv \beta f_{aPPFD} \sum_d \Phi_d \prod_i f_{id} \quad (1)$$

where f_{aPPFD} is the fraction of photosynthetic photon flux absorbed by the canopy, P_0 is the potential photosynthetic production when all radiation is absorbed ($f_{aPPFD} = 1$), β is the potential light use efficiency (gC mol^{-1}, Table 1), Φ_d is photosynthetic photon flux density of day d (PPFD, mol m^{-2} day^{-1}), and f_{id} are values on day d of environmental modifiers related to variable i ($i = L, S, D, W$ representing light, temperature, vapour pressure deficit and soil water, respectively). The product of Φ and the light modifier f_L takes the form of rectangular hyperbola, which describes the saturating light effect on stand P, the temperature modifier f_S calculates the seasonal temperature potential for P. It is calculated using daily mean temperatures and over the course of the year the response typically takes a form resembling a cut sine wave where the peak values during summer are flattened to 1, while during the off-season (currently November-March in southern-most

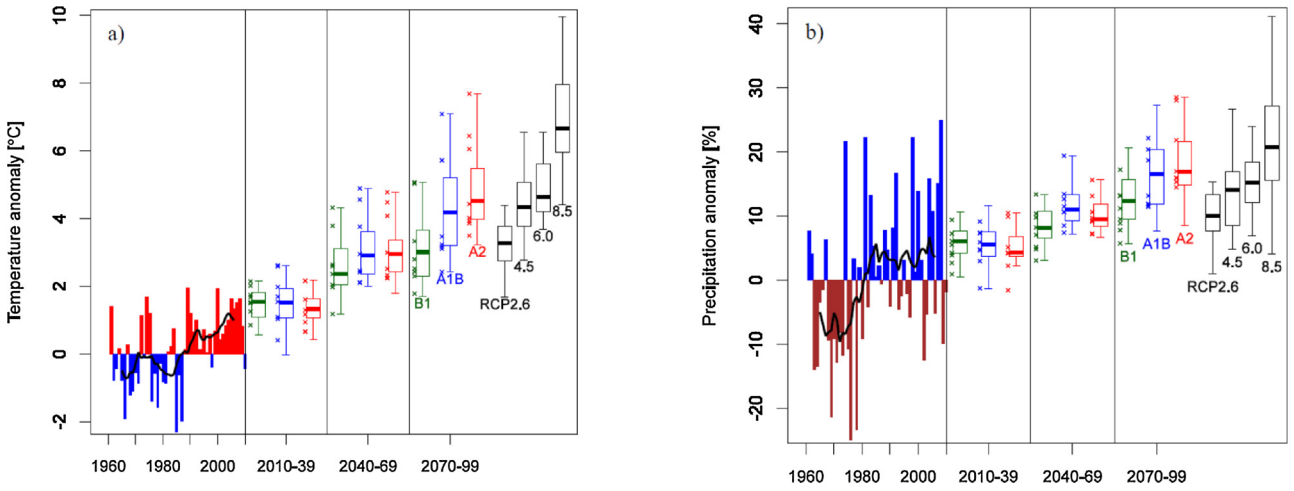

Fig. 1. Observed anomalies in average annual (a) air temperature and (b) precipitation and projected changes for 30-year mean periods during the 21st century for Finland for SRES scenarios B1, A1B and A2 simulated with 8 GCMs selected for this study (stars) and for the full ensemble of 24 Coupled Model Intercomparison Project phase 3, CMIP3, models (boxplots), modified from Rötter et al. (2013). GCMs are listed in Table SA.1 in the supplementary material. Similar projected changes for RCP scenarios projected by CMIP5 GCMs are shown for last 30-year period.

Table 1
Definition of tree species using model parameters. All other parameters were kept as defaults (Peltoniemi et al., 2015).

Tree species	Effective soil water holding capacity[a]	κ[b]	β[c]	
Pine	167	0.13	0.75	Parameter set from Hyytiälä eddy-site that compared well with Sodankylä eddy-covariance site parameterization.
Spruce	210	0.4	0.75	
Birch	260	0.4	0.94	

[a] The column height (mm) of extractable soil water roots of the trees have access to.

[b] Parameter of VPD sensitivity f-modifier, $f_D = e^{-\kappa D}$.

[c] Deciduous species have clearly higher foliar [N] than conifers, which promotes higher β (Peltoniemi et al., 2012). Deciduous species LUE were predicted assuming a linear relationship between LUE and (Peltoniemi et al., 2012) mean needle N concentration (1.27 mg N (gDM)$^{-1}$ for pine and 2.40 mg (gDM)$^{-1}$ for birch, updated dataset of Merilä and Derome 2008). Mean pine needle N concentration in this dataset was assumed to generate the LUE estimated for Hyytiälä.

Finland) there is marginal or no potential to photosynthesize and its values are zero or close to zero. Impacts of the water vapor pressure deficit of atmosphere, D (VPD), and soil moisture, are implemented as $f_{D,W} = \min(f_D, f_{W,P})$. Here, f_D describes a modest exponential decrease of P with increasing D, and $f_{W,P}$ describes the decrease of photosynthesis with decreasing soil moisture content (Table 2 and Table 1 in Appendix A).

In order to calculate $f_{W,P}$, soil water balance and relative extractable water (W) are predicted using a simple bucket model where the water balance is controlled by precipitation, evapotranspiration, snowmelt, throughfall, and drainage. The modifier $f_{W,P}$ is then defined as $f_{W,P} = \min(1, W/\rho_P)$, i.e., low W below fitted parameter ρ_P thus potentially decreases $f_{D,W}$. The simple soil water model does not describe lateral water flows, except that, above field capacity (θ_{FC}), a fraction of water is lost as runoff every day and becomes inaccessible to roots.

Evapotranspiration (E) is predicted using an empirical model, which is sensitive to P prediction, D, Φ, temperature, and f_{aPPFD}.

$$E = \alpha P f_{W,P}^{\nu} D^{1-\lambda} + \chi(1-f_{aPPFD})\phi f_{W,E} \quad (2)$$

where parameters α, ν, λ and χ are fitted parameters, which partially determine the fraction of the two water fluxes (the two components of the sum, Eq. (2)) that correspond to transpiration and evaporation. The modifier $f_{W,P}$ of the P equation is raised to the power ν because P and E fluxes are not similarly influenced by drought. Modifier $f_{W,E}$ reduces evaporation under dry soil; formulation of $f_{W,E}$ modifier follows $f_{W,P}$ but has its own (fitted) threshold ρ_E, i.e. $f_{W,E} = \min(1, W/\rho_E)$. The model also includes a storage for surficial water (θ_{surf}) and snow (θ_{snow}), which are accounted for in the stand water balance. If $\theta_{surf} > 0$ or $\theta_{snow} > 0$ then $f_{W,E} = 1$.

For incorporating the CO_2 response in the model, the C_a effects on

Table 2
Parameters sampled from the posteriori of Peltoniemi et al. (2015) and their ranges used in the simulations.

Parameter	Symbol	Unit	Used range
Potential light use efficiency	β_P	g C mol^{-1} m^{-2}	0.685…0.810
Delay parameter for the response of temperature acclimation state to the changes in ambient temperature	τ	–	11.43…15.74
Threshold above which the state of acclimation increases	X_0	°C	−4.56…-2.97
Threshold at which the acclimation modifier reaches its maximum	S_{max}	°C^{-1} d^{-1}	17.75…20.08
Sensitivity parameter of fD to D	κ	kPa^{-1}	−0.196…-0.070
Light modifier parameter for saturation with irradiance	γ	mol^{-1} m^{-2}	0.029…0.041
Threshold for W effect on P in modifier fW,P	ρ_P	–	0.397…0.902
Transpiration parameter	α	mm (g C m^{-2} kPa1 − λ)$^{-1}$	0.308…0.358
Parameter adjusting transpiration with D	λ	mol^{-1} m^{-2}	0.100…0.919
Evaporation parameter	χ	mm mol^{-1}	0.023…0.059
Threshold for W effect on evaporation in modifier fW,E	ρ_E	–	0.0002…0.9983
Parameter adjusting transpiration with W	ν	–	0.013…0.685
Surfacial water storage maximum	$\theta_{surf,max}$		0.422…5.000

stand P were estimated using summary functions emulating the SPP stand photosynthesis model with Farquhar equations (Farquhar et al., 1980; Leuning, 1995) for leaf photosynthesis (Mäkelä et al., 2006; Kolari et al., 2009). The SPP model simulations were done with using the SMEAR II stand as representative of typical middle-aged managed Scots pine stand (see Ilvesniemi et al., 2009 for detailed description of the site and stand structure).

The C_a influences both P and E through their own modifiers. The effects of soil moisture are partially influenced by C_a.

P is influenced by CO_2 of air in two ways. Firstly, if ambient CO_2 increases above its reference level $C_{a,ref}$, the photosynthetic efficiency will increase in a nonlinear manner which is described with the following modifier function:

$$f_{CO_2,P_0} = 1 + \frac{C_a - C_{a,ref}}{C_a - C_{a,ref} + C_{Sat}} \quad (3)$$

At the same time, however, the VPD response is also altered by decreasing the slope of the VPD response in increasing C_a due to partial closure of stomata, described as follows:

$$f_{CO_2-D} = e^{\chi_f \left(\frac{C_{a,re}}{C_a}\right)^{0.4} \cdot D} \quad (4)$$

Finally, the above reponses are combined in the following CO_2 modifier of photosynthesis:

$$f_{P,\,CO_2} = f_{CO2,P0}\, f_{CO2\text{-}D} / f_D. \quad (5)$$

which describes the overall effect of C_a on photosynthesis.

The evapotranspiration, E, is also influenced by CO_2. Implementation of E changes under changed CO_2 concentration was made with a multiplier modifying the transpiration, i.e the first part of the model function for E (see Eq. (2) above):

$$f_{Tr,CO_2} = 1 - \frac{C_a - C_{a,ref}}{C_a - C_{a,ref} + C_{Sat}} \quad (6)$$

For more details, consult Mäkelä et al. (2008a,b), Peltoniemi et al. (2015) and Minunno et al. (2016).

2.2. Standard set of model parameters

A standard set of parameters at reference C_a was obtained from the previous Scots pine stand parameterisation (Peltoniemi et al., 2015). The parameterisation under changing C_a was based on this reference case and the simulations of relative changes in the more detailed SPP model, as explained above (Table 1).

We further modified these pine (*Pinus sylvestris* L.) parameters on the basis of the literature (Mäkelä et al., 2008a,b; Linkosalo et al., 2008; Minunno et al., 2016) to represent Norway spruce (*Picea abies* [L.] Karst.) and silver birch (*Betula pendula* Roth.) in the analysis (Table 1). In Minunno et al. (2016), the authors found no significant differences in the parameter estimates between Scots pine and Norway spruce dominated stands. Because spruce and birch generally occupy moister sites than pine, we increased the soil water holding capacity for them. The aim was to provide a realistic description of the typical growth sites of the different species. In addition, the parameter modifications assumed that spruce and birch had higher sensitivity to D than pine. Birch also has a higher light-use efficiency than pine and spruce (Peltoniemi et al., 2012). A description of the phenology of leaf budburst for birch was adopted from Linkosalo et al. (2008). This phenology model is an on-off variable which determines the date on which the temperature modifier f_S is activated. The phenology model does not account for autumn phenology, i.e. there is no description of leaf-senescence and its potential effect on photosynthesis.

The fraction of absorbed photosynthetic photon flux density, f_{aPPFD}, essentially depends on forest structure. To screen the impact of structure on P we used three values (0.5, 0.75, and 1, Figs. SB.1–SB.3), representing sparse, typical and theoretical stands that harvest different proportions of PPFD. The f_{aPPFD} also has a minor impact on the total amount of evapotranspiration and on the ratio of transpiration to evaporation.

2.3. Estimating PRELES parametric uncertainty

For estimating the parametric uncertainty of the impact model, we used a posterior distribution of parameters obtained with Bayesian inversion, and by applying the above adaptive Markov Chain Monte Carlo (MCMC) algorithm in the model calibration study (Peltoniemi et al., 2015). We used the differential evolution Markov chain (DEMC, ter Braak (2006)) algorithm to sample from the posterior distribution. The algorithm combines a global optimization algorithm, the differential evolution method of Storn and Price (1997), with an MCMC simulation step. A few Markov chains are run in parallel learning from each other. We used the DEMC version (ter Braak and Vrugt, 2008) that uses a reduced number of chains (3) and a snooker updater implemented in the R package BayesianTools (Hartig et al., 2017). Here we varied 13 parameters of the posteriori (Table 2).

We deemed 60 posteriori samples sufficient for characterizing the uncertainty of model parameters, their co-variation, consequent predictions of the model, as well as the distribution characterizing the distribution of residuals. The subset of the parameter vectors used in the simulations was sampled with even sized step from the posteriori distribution in such a manner that the whole parameter space formed by the posteriori was sampled. Fig. SB.5 shows how the obtained subset covers the total variation of posteriori distribution of each parameter. The uncertainty of the mean response of the model (i.e. daily P) was generated using model parameters in the posterior sample. The uncertainty attributed to model parameters only partially captures the uncertainty of daily P. Around the mean response, there is variation of residuals, which stems from the uncertainties of observations used in the model calibration and inability of the model structure to describe the true variation. Therefore, for each day of the year in each simulated run, we drew a sample from the normal distribution with standard deviation s, centered on the simulated P for that day. Values of s were specific to the model parameters used; they were obtained from the same posterior sample as model parameters.

2.4. Structural uncertainty

The largest structural uncertainty of the model is related to the increased WUE due to C_a fertilization effect. The C_a effect was added to the model on the basis of a more detailed model (cf. Kolari et al., 2009), while the other environmental effects have been calibrated against data (Minunno et al., 2016). To quantify this uncertainty, we explored four alternative assumptions. Firstly, we assumed a full impact of the model described above, implying direct effects on photosynthesis and evapotranspiration and indirect effects on soil moisture through effects on evapotranspiration. Secondly, we assumed no effect on soil moisture, because it is possible that any reduction in transpiration due to C_a effects could be counteracted by increased evaporation (Allen et al., 2010). Thirdly, some studies have indicated a strong downregulation of photosynthesis even if C_a increases (Ellsworth et al., 2004); we therefore considered the possibility that C_a influences neither P nor evapotranspiration. Finally, we considered the hypothetical case that there was no effect of C_a on P and that soil moisture did not affect the processes at all. In this case, all effects are primarily caused by temperature increase.

These assumptions gave rise to the following model settings:

1 All factors

The full model, including the effects of daily mean temperature (T, °C), vapor pressure deficit (D, kPa), photosynthetic photon flux density

above the canopy (ϕ, mol m^{-2}), C_a (ppm) and effective rooting zone soil water (θ, mm).

2 All factors less soil water: the case *–soil water*

The effects of soil moisture constraint on P were removed, i.e. we set the soil water modifier in the model, $f_{W,P}$, to unity.

3 All factors less C_a: the case $-C_a$

Here $C_a = C_{a,\,ref}$, which forces the $f_{P,CO2}$ and $f_{E,CO2}$ modifiers to 1.

4 All factors less soil water and C_a: the case $-CO_2$ *–soil water*

Here $C_a = C_{a,\,ref}$, and constraints of soil moisture on P through soil water deficit were removed.

2.5. Input uncertainties: baseline and future climate data

Baseline daily weather data on a regular 10 km × 10 km grid covering Finland for the period 1971–2000 were obtained from the Finnish Meteorological Institute for mean temperature, precipitation, global radiation and vapour pressure (Venäläinen et al., 2005). The estimation of PPFD and VPD from these data is described in Suppl. A. Climate scenarios for the 21st century were prepared by downscaling GCM simulations of the SRES emission scenarios (IPCC, 2007) and the more recent Representative Concentration Pathways (RCPs, IPCC et al., 2013) that took part in the Coupled Model Intercomparison Project (CMIP) phases 3 (for SRES, Meehl et al., 2007) and 5 (for RCP, Moss et al., 2010). Subsets of the full CMIP3 and CMIP5 ensembles were selected for which the required set of variables was available and which we regarded as representative for spanning the range of projected changes in the full ensembles. The criteria for representative ensembles were that they covered a sufficient range of uncertainty from a larger ensemble, and that the biases between the historical simulation and observed climate were not judged to be too large (Ruosteenoja et al., 2011). For the SRES-based scenarios, eight GCM simulations of the B1, A1B and A2 emission scenarios were selected (cf. Fig. 1 and Rötter et al., 2013). For RCP-based scenarios, 5 GCMs were selected, all covering the low RCP2.6, moderate RCP4.5 and high RCP8.5 forcing scenarios (Suppl. A Fig. SA.1, IPCC et al., 2013).

Two alternative downscaling approaches were used: a simple change factor approach for the SRES simulations and bias-adjustment for the RCP simulations.

In the change factor approach, simulated monthly long-term changes in climate variables for the periods 2011–2040, 2041–2070 and 2071–2100 relative to 1971–2000 (Suppl. A Table SA.1) were used to adjust daily observed time series. The GCM grid cell centre point values were re-projected to the projection of the grid of the observed database and monthly changes were bi-linearly interpolated to estimate values for the centre points of the 10 × 10 km grid cells. For each grid cell, monthly changes were linearly interpolated to daily changes, which were added to the observed time-series. The development of C_a during 21st century was taken from simulations with the BERN carbon cycle model (Suppl. A Fig. SA.1, IPCC, 2007). It is also assumed that the climate model bias remains the same in the simulations of future climate (Ruosteenoja et al., 2011). For further illustrations of the climate scenarios see Supplement A and details of the construction of climate scenarios see Rötter et al. (2013).

The dataset obtained from Finnish Meteorological Institute consisted of RCP-based simulations of climate input variables for the period 1980–2100. These data were bias-adjusted with observed daily data (Aalto et al., 2013) on a 10 × 10 km grid over Finland using quantile mapping (Suppl. A). The bias-adjusted model output was interpolated, using the bilinear method, onto a 10 × 10 km grid covering the area of Finland.

The bias-adjusted simulations represent a transient time-series from 1980 to 2100, whereas the SRES-based scenarios are not strictly a continuous, transient time-series, but 30-year time-series separate for baseline and three future periods.

2.6. Decomposition of sources of uncertainty

We estimated the uncertainty of GPP and ET projections arising from the impact model (parametric and structural uncertainty) and its weather inputs (scenario, climate model variation). The analysis was done separately for the RCP emission pathways and SRES emission scenarios.

We had $S = 3$ emission descriptions either in RCP (RCP2.6, RCP4.5 and RCP8.5) or SRES (A2, A1B, B1). For producing the climate projections we had an ensemble of $M = 5$ GCMs (CMIP5) for RCP and $M = 8$ GCMs (CMIP3) for SRES. We also included the parametric uncertainty of impact model ($K = 60$ parameter vectors). The parameter vectors were the same for both RCP and SRES analyses. For each year t we therefore calculated $S \times M \times K$ values of the predicted variable, i.e. annual mean GPP or ET value, denoted by x^t_{ksm}. The total variation could be described as a set of values, X^t, for each year:

$$X^t = \{x^t_{kms} k = 1,...,K;\ m = 1,...,M;\ s = 1,...,S\} \quad (7)$$

Here s is either concentration pathway in RCP or SRES emission scenario, m is GCM, and k is parameter vector of PRELES. We then reduced the variation in three steps. First, we calculated the average over parameter vectors for each scenario and climate model and year, yielding values denoted by $x^t_{\bullet ms}$ and defining the set X^t_k:

$$X^t_k: =\{x^t_{\bullet ms} m = 1,...,M;\ s = 1,...,S;\} \quad (8)$$

The variability in X^t_k is therefore smaller than the overall variability, and the difference is accountable to parameter uncertainty. Similarly, we averaged these over the GCMs, yielding

$$X^t_{km}: =\{x^t_{\bullet\bullet s} s = 1,...,S\} \quad (9)$$

The difference between X^t_{km} and X^t_k accounts for the GCM uncertainty. Finally, we defined the following overall annual mean:

$$\hat{x}_t = \frac{1}{S} \times \frac{1}{M} \times \frac{1}{K} \sum_k \sum_m \sum_s x^t_{kms} \quad (10)$$

The variability around the mean created by X^t_{km} accounts for variability in concentration pathway/emission scenario.

We then found minima and maxima in the sets X^t, X^t_k, and X^t_{km} for all years t. Combined with the overall mean, this procedure gave us seven time series over the simulation period. We assumed that these time series described the different components of variability in our predictions. We further fitted smooth time functions to these discrete time series using linear functions or log-log transforms. For estimating the natural variability of climate, we used the reference period (1980–2010) as a basis.

The above method for decomposing the uncertainty is descriptive and does not account for possible interactions between the components. We therefore followed the approach of Nishina et al. (2015) and carried out a three-way analysis of variance (ANOVA) for the annual GPP / ET for describing the relative importance of the different sources of variation and their interactions as

$$SS_{overall_t} = SS_{s_t} + SS_{m_t} + SS_{k_t} + SS_{s\times m_t} + SS_{s\times k_t} + SS_{m\times k_t} + SS_{s\times m\times k_t} \quad (11)$$

in which t is year. $SS_{overall}$ is the total variability around the mean (sum of squares), and the other symbols are as above. Here we also considered interaction effects between the components. We did this analysis of decomposing uncertainty only for one grid point (10 km × 10 km) corresponding to the location of Hyytiälä Forest station (southern Finland; 61°50.845 N, 24°17.686E, 181 m a.s.l.).

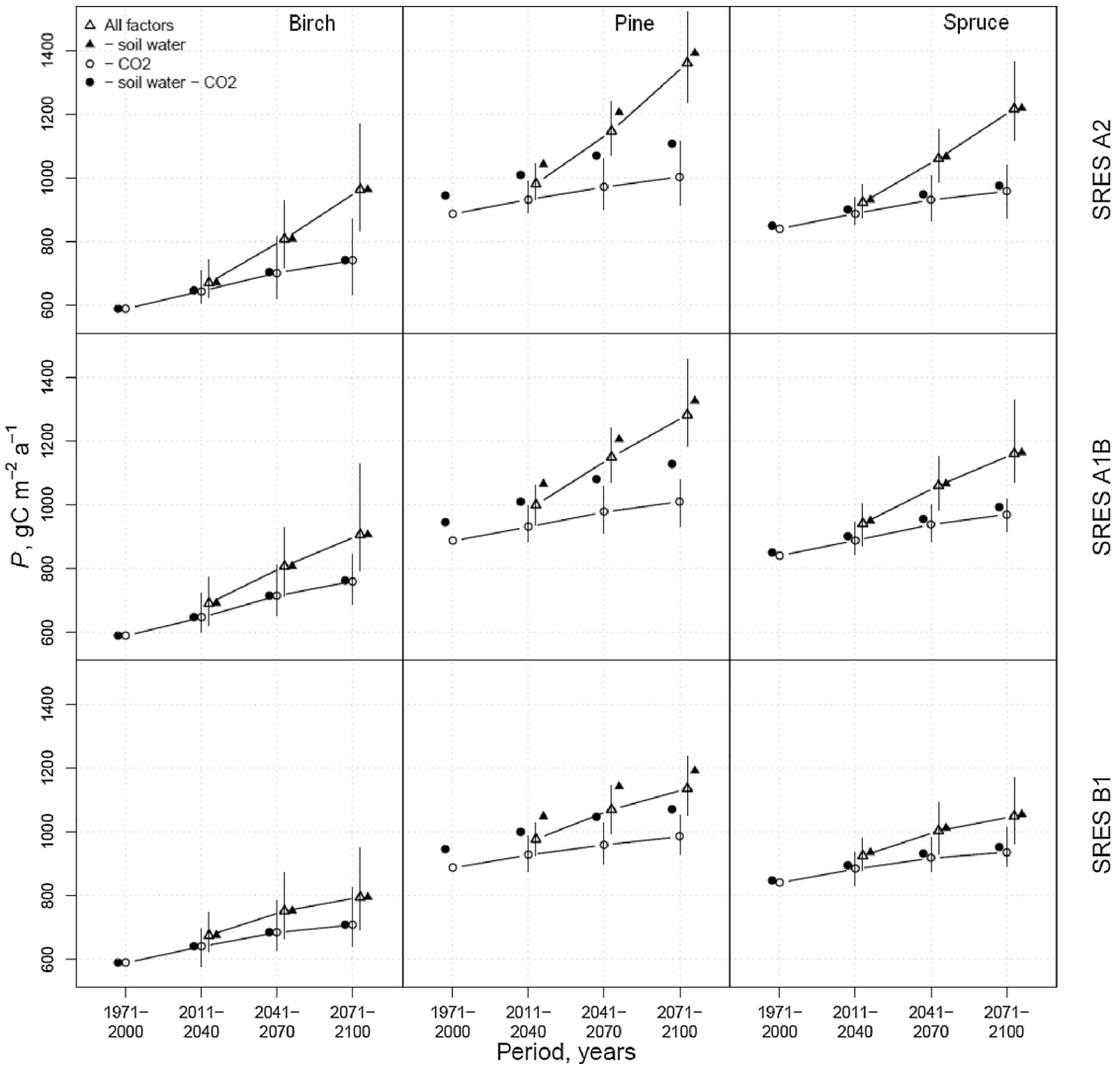

Fig. 2. Effect of climate change on gross primary production (*P*) of forests in Finland with the fraction of absorbed photosynthetic photon flux density (f_{aPPFD}) 0.75. Symbols show the mean prediction obtained using the downscaled projections of eight CMIP3 global circulation models in different SRES emission scenarios. Horizontal lines connect the symbols of "All factors" and "$-CO_2$" simulation cases (see Section 2.4). Vertical lines show the range of predictions obtained with these projections (min – max), for clarity only for the same two simulation cases as in case of horizontal lines.

3. Results

3.1. Projections of GPP and ET for SRES-based climate scenarios

Climate change increased the species specific ensemble mean GPP in all simulation cases (cf. Section 2.4) within all SRES scenarios and the magnitude of the changes followed the projected emissions in the scenarios, being largest in A2 (in average 36%) and lowest in B1 (25%), while A1B was closer to A2 (Fig. 2). The predicted GPP driven with projections of SRES and CMIP3 ensemble had a large range which nearly corresponded to the change itself (relative range was 88% across scenarios at the end of the period, Table 3). Considering the structural uncertainty, the C_a fertilization effect alone was decisive for the overall impact on GPP in all species, regardless of what was assumed about soil moisture (Fig. 2, Table 3).

If C_a fertilization effect was excluded (Section 2.4, case 3.) and species pooled the average GPP increase was almost the same in A2 (19%) and A1B (18%) and only slightly smaller in the B1 (14%) scenario. Therefore, in B1 the ensemble range was much larger relative to the mean change itself (170%), meaning that the most conservative climate change predictions yielded only conservative increases of GPP by the end of the century.

Changes of other climatic factors, mostly temperature, also increased GPP in all scenarios (Fig. 2, black filled circles). In the climate model projections with the largest increases in temperature, the effects of other climatic factors roughly equalled those of C_a (Table 3). The minimum GPP estimates in B1 suggested that without the C_a effect, none of the species would benefit from climate change during the first simulated period 2011–2040 (Fig. 2).

Most of GPP increases can still be attributed to the increases of GPP in summer (May-Aug). Increases of GPP in the winter-spring period (Jan–Apr) were approximately as high as increases of GPP in autumn (Sep–Dec), suggesting that summer season radiation conditions dominate as drivers of annual GPP increase (data not shown).

In the climate projections, the change in precipitation was less pronounced than change in e.g. temperature (Fig. 1). Anyhow, the soil water constraint was relaxed due to decreasing transpiration in the conifers (Fig. 3). This effect was clearest in pine which was the species most constrained by soil water in reference climate due to low soil water holding capacity. This effect was only slight in spruce, while birch GPP was not affected by soil moisture deficit in any of the time periods in any SRES emission scenario. When the C_a effect was excluded, the increased evapotranspiration exceeded the effect of larger rainfall and thus, GPP of pine was more constrained by soil water deficit

Table 3
Changes of gross primary production (P, g C m^{-2} a^{-1}) with default parameter set of PRELES and the downscaled projections of the ensemble of eight CMIP3 -GCMs over Finland separately in SRES B1, A1B and A2 scenario with the fraction of absorbed photosynthetic photon flux density (f_{aPPFD}) 0.75.

Species	Scen	Case	Period	Mean	Max	Min	Relative		
							Mean	Max	Min
Birch	B1	All_factors	2011-2040	676	748	625	0.17	0.30	0.09
			2041-2070	752	873	665	0.31	0.52	0.16
			2071-2100	795	948	694	0.38	0.65	0.21
		No_CO2	2011-2040	641	696	576	0.09	0.18	−0.02
			2041-2070	685	785	630	0.16	0.33	0.07
			2071-2100	709	826	643	0.20	0.40	0.09
	A1B	All_factors	2011-2040	691	773	621	0.20	0.34	0.08
			2041-2070	807	930	714	0.40	0.62	0.24
			2071-2100	907	1129	795	0.58	0.96	0.38
		No_CO2	2011-2040	646	723	602	0.10	0.23	0.02
			2041-2070	715	809	651	0.21	0.37	0.10
			2071-2100	760	846	687	0.29	0.44	0.17
	A2	All_factors	2011-2040	671	741	623	0.17	0.29	0.08
			2041-2070	808	930	718	0.41	0.62	0.25
			2071-2100	964	1168	834	0.68	1.03	0.45
		No_CO2	2011-2040	645	710	608	0.09	0.21	0.03
			2041-2070	702	817	622	0.19	0.39	0.06
			2071-2100	741	871	634	0.26	0.48	0.08
Spruce	B1	All_factors	2011-2040	925	979	880	0.13	0.20	0.07
			2041-2070	1003	1094	931	0.22	0.34	0.14
			2071-2100	1050	1169	964	0.28	0.43	0.18
		No_CO2	2011-2040	884	935	831	0.05	0.11	−0.01
			2041-2070	918	984	876	0.09	0.17	0.04
			2071-2100	937	1013	891	0.11	0.21	0.06
	A1B	All_factors	2011-2040	941	1002	873	0.15	0.22	0.07
			2041-2070	1060	1154	984	0.29	0.41	0.20
			2071-2100	1161	1328	1072	0.42	0.62	0.31
		No_CO2	2011-2040	888	948	844	0.06	0.13	0.00
			2041-2070	938	1002	886	0.12	0.19	0.05
			2071-2100	970	1016	915	0.15	0.21	0.09
	A2	All_factors	2011-2040	923	981	875	0.13	0.20	0.07
			2041-2070	1061	1153	985	0.29	0.41	0.20
			2071-2100	1217	1366	1117	0.49	0.67	0.36
		No_CO2	2011-2040	888	937	854	0.06	0.12	0.02
			2041-2070	931	1008	865	0.11	0.20	0.03
			2071-2100	958	1042	875	0.14	0.24	0.04
Pine	B1	All_factors	2011-2040	977	1027	926	0.14	0.20	0.08
			2041-2070	1070	1146	996	0.25	0.34	0.16
			2071-2100	1136	1238	1052	0.33	0.45	0.23
		No_CO2	2011-2040	928	986	874	0.05	0.11	−0.01
			2041-2070	959	1029	898	0.08	0.16	0.01
			2071-2100	985	1052	928	0.11	0.19	0.05
	A1B	All_factors	2011-2040	1000	1061	935	0.17	0.24	0.09
			2041-2070	1150	1242	1070	0.34	0.45	0.25
			2071-2100	1283	1458	1184	0.50	0.70	0.38
		No_CO2	2011-2040	931	999	886	0.05	0.13	0.00
			2041-2070	977	1057	913	0.10	0.19	0.03
			2071-2100	1010	1080	931	0.14	0.22	0.05
	A2	All_factors	2011-2040	981	1044	932	0.15	0.22	0.09
			2041-2070	1147	1239	1070	0.34	0.45	0.25
			2071-2100	1361	1520	1238	0.59	0.78	0.45
		No_CO2	2011-2040	932	989	890	0.05	0.12	0.00
			2041-2070	971	1059	902	0.10	0.19	0.02
			2071-2100	1004	1115	915	0.13	0.26	0.03

in all SRES scenario climates than in the reference period (Fig. 3). In spruce this effect was much less pronounced and in birch it could not be detected.

The increase of GPP was in absolute terms only slightly larger in southern than in northern Finland in all simulated SRES cases. Relative increases were thus higher in the north in all modelled species and the range of GPP predictions was also larger in northern than in southern Finland (Fig. 4).

The relative change in GPP was the highest in birch in North Finland, up to 80% (44%–127%) in the A2 scenario at the end of the century (Table 3). Larger increases of GPP in birch than in other species were predominantly caused by a stronger effect of the temperature increases. This was illuminated by the result that when C_a fertilization effect (case 3.) was excluded the changes were still the most pronounced for birch, 33% (7%–69%, Table 3).

3.2. Contribution of different uncertainty sources to GPP and ET

In absolute terms, the overall uncertainty increased greatly over time both in GPP and ET and differed clearly between SRES and RCP simulations (Figs. 5 and SA.5). However, the pattern of the GPP in terms of the fraction of uncertainty for each variable was quite similar in both (Fig. 6). The year to year variation was large being ca. 55% in SRES and 48% in RCP and could be detected even in smoothed five

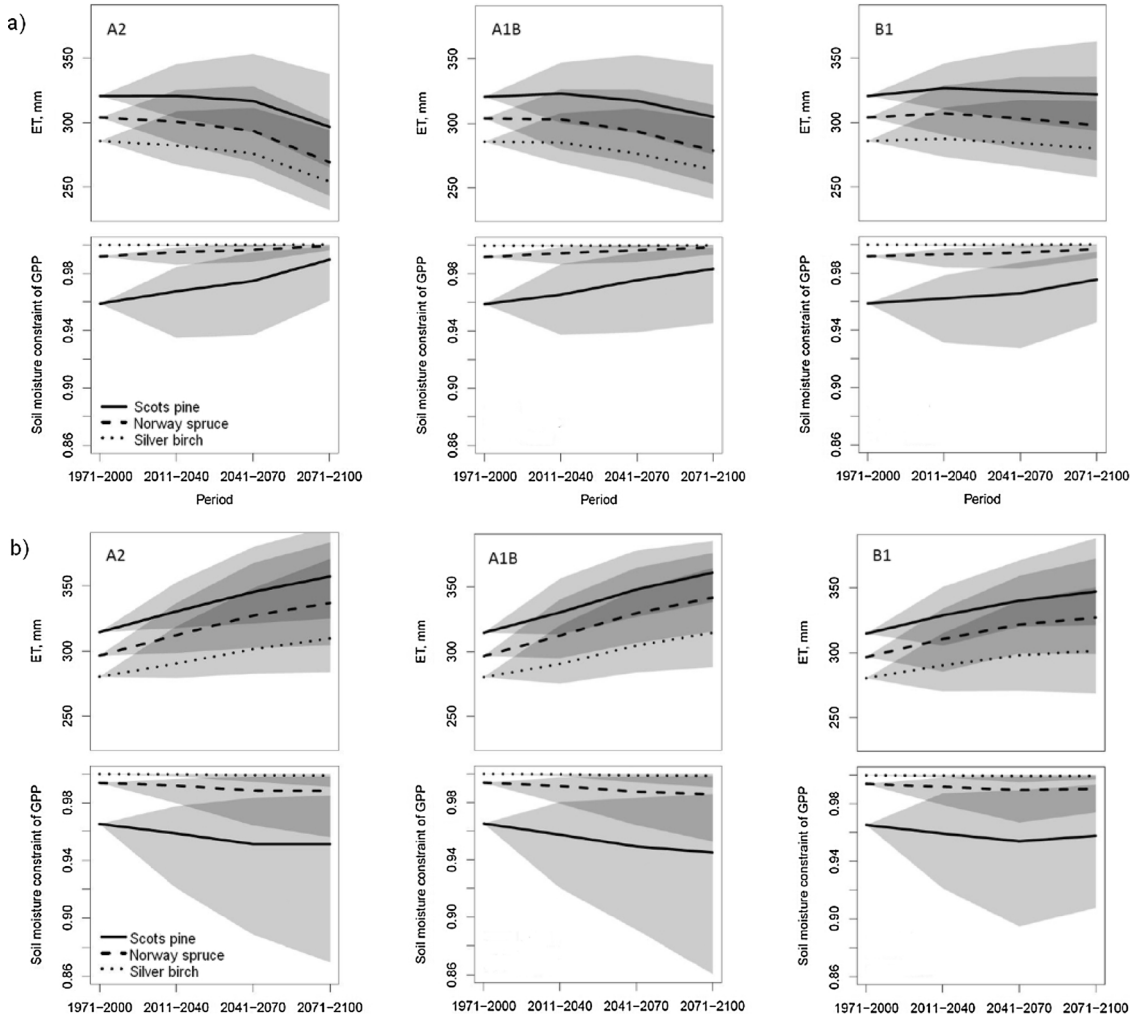

Fig. 3. Simulated evapotranspiration *E* and soil moisture constraint in SRES scenarios during 21st century in simulation cases A) '*All factors*' and B) '*All factors less* C_a'. The gray-shaded bands are the range of the response variable obtained with the downscaled projections ofeight CMIP3 GCMs in different SRES scenarios.

years average (Fig. 6). The relative importance of the different sources of uncertainty changed over time in both the predictions of GPP and ET. For GPP, the GCM uncertainty dominated roughly before 2060 and emission uncertainty thereafter. For ET, GCM uncertainty remained the largest throughout 21st century in SRES while RCP emission uncertainty exceeded that of GCMs only around 2080. In GPP of the SRES, the emission uncertainty never exceeded the natural variability while in RCP this occurred already around 2060 (Fig. 5). A significant interaction effect between emission scenario uncertainty and GCM uncertainty was found for SRES but not for RCP. The uncertainty due to PRELES parameters was almost negligible in predictions of GPP but much larger in the predictions of ET in both SRES scenarios and RCP pathways. In ET also, the dominant role of variation between GCMs was eminent (Fig. 6).

4. Discussion

The starting point for any model based analysis of the carbon cycles is the reliable description of gross primary production. We covered a broad envelope of predictions, multiple GCMs and multiple emission scenarios with one impact model, allowing us to make conclusions on the types of change that seem likely for different species or sites. Moreover, our results revealed the sensitivity of predictions of the PRELES model to input uncertainty and how the variability of GPP and ET propagates from emissions scenarios to the assumptions of the impact model CO_2 response function. The most general finding was that the selection of the climate change projection had a profound influence on both the predicted GPP and ET of boreal forests of Finland. Many studies concerning different ecological impacts of climate change, e.g. disturbances (e.g. Lehtonen etal. 2016, Seidl et al., 2017) have noted this. We considered here a continuous variable whereas disturbance is always discrete which emphasizes the need for specific analysis for different impacts. However, in both cases the wide range of projections may lead to difficulties in drawing ecologically meaningful conclusions (Cavanagh et al., 2017). Real uncertainty is even larger due to feedback loops between climate and vegetation (e.g. Forzieri et al., 2017) which we could not account for with a simple tool like PRELES.

The highest predictions of GPP were almost double compared with present day observations, while the lowest predictions without C_a fertilization effect did not increase GPP during the next decades and barely during the whole century. The species specific mean GPP increased in all simulated cases and was generally in the same scale as found in earlier studies with more mechanistic models (Wamelink et al., 2009; Ge et al., 2013; Reyer et al., 2014). Our finding that the decomposition of uncertainty hardly differed between combinations of older SRES emission scenarios and CMIP3 projections and the currently used RCPs and CMIP5 GCMs lends support to the robustness of this result. The difference of the climate projections for Finland between SRES and RCP scenarios seems to be quite modest (Fig. 1) especially if compared with the high variability between projections of individual GCMs (Fig. 6). Thus, from the viewpoint of forest impact studies SRES and RCP projections essentially cover the same range (van Vuuren and Carter,

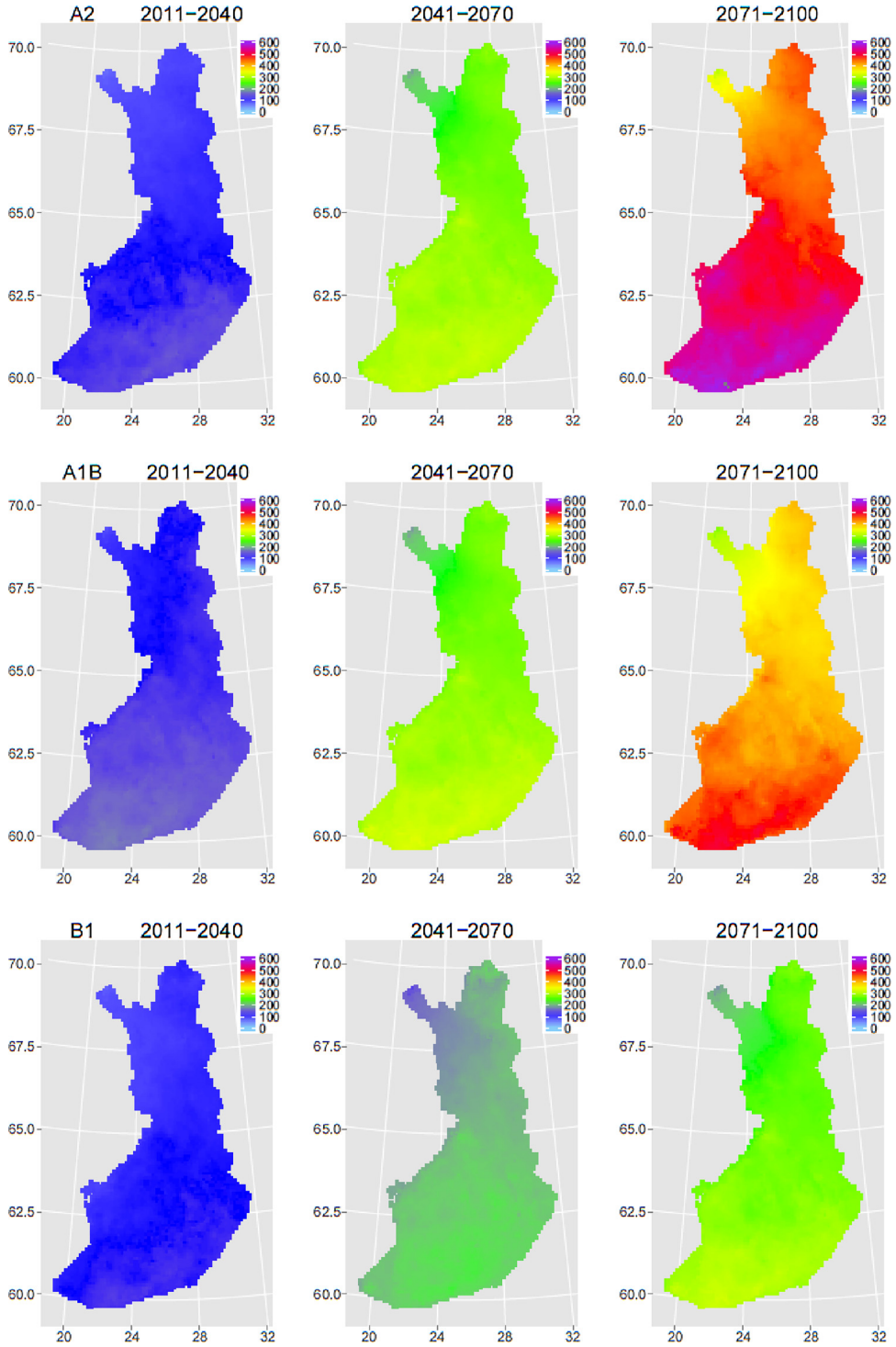

Fig. 4. The range of change of gross primary production (P, g C m^{-2}) predictions for Scots pine in simulation case '*All factors*' with the downscaled projections of the ensemble of eight CMIP3 8-GCMs and with faPPFD = 0.75 in the different SRES emission scenarios.

2014). Our results were consistent with earlier studies in the sense that GCMs were the dominant sources of uncertainty for GPP until around 2060, while uncertainty of the temporal development of emissions, either driven by RCP or SRES scenarios, dominated later in the projection period (2060–2100, Nishina et al., 2015; Horemans et al., 2016). We note that this uncertainty analysis only covered one grid point (Hyytiälä forest station), but extending it to the whole country would likely not create more than marginal changes to the decomposition of uncertainty, due to the small parametric variation in PRELES.

The difference of variation between RCP and SRES observed here was partly due to the fact that selected pathways of RCPs were more extreme than emission scenarios of SRES (RCP2.6 vs SRESB1 and RCP8.5 vs SRESA2). In addition, GCMs have developed from CMIP3 to CMIP5. However, although characteristics of the CMIP5 models have changed from CMIP3, e.g. they may have higher resolution, their atmospheric or ocean components may have changed in order to improve their ability to describe the fluxes between ecosystems and the atmosphere, the models in the new ensemble are neither independent of each other nor independent of the earlier generation (Knutti et al.,

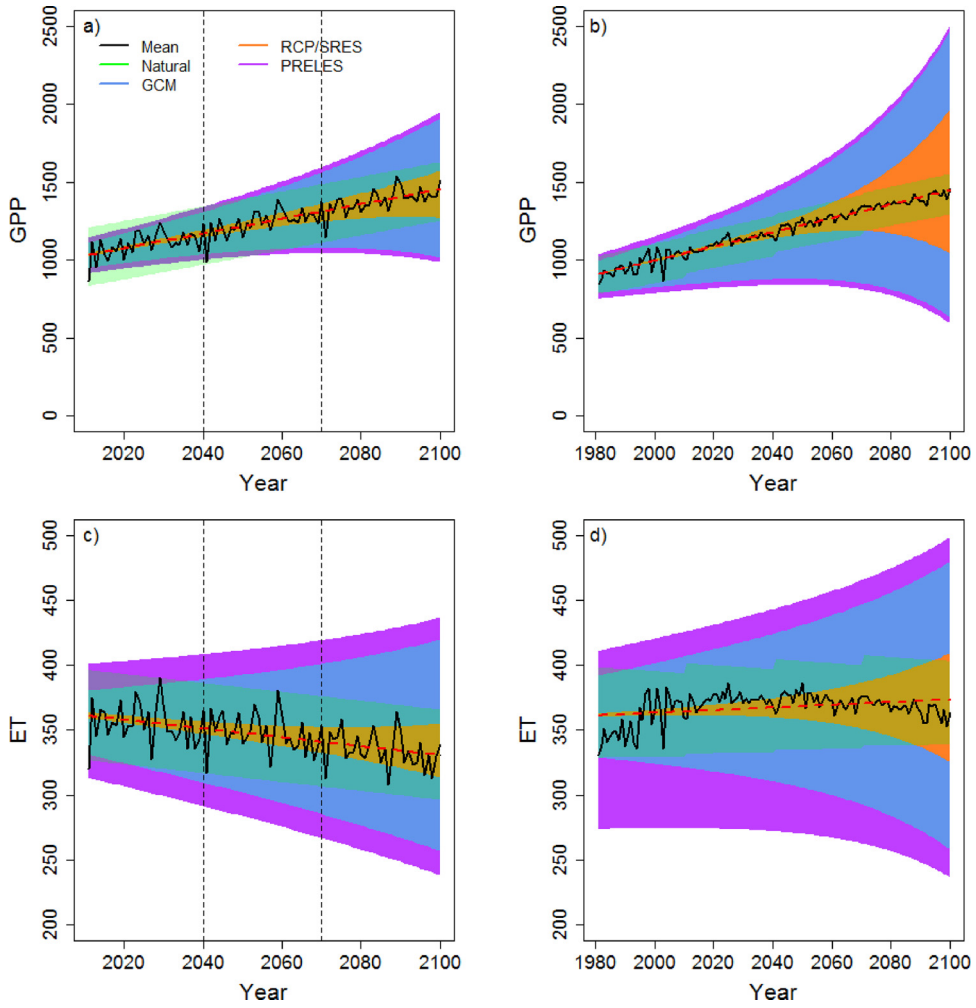

Fig. 5. Role of different sources of uncertainty (see Eqs. (7)–(10)) on the predicted Scots pine GPP and ET in one grid cell (Hyytiälä Forest Station). The different colors are additive and total uncertainty ($S \times M \times K$) is illustrated by total colored area. The colors indicate removing one source of uncertainties stepwise, starting from PRELES parametric and structural uncertainty (purple area, $K = 60$ parameter vectors, same vectors for both RCP and SRES), GCM variability (blue area, $M = 5$ CMIP5 GCMs for RCP and $M = 8$ CMIP3 GCMs for SRES), and emission pathways/scenarios (orange area, $S = 3$ emission descriptions separately for RCP [RCP2.6, RCP4.5, RCP8.5], and SRES [A2, A1B, B1]). The lighter colour in the middle indicates the natural climatic variability. a) GPP in SRES, b) GPP in RCP, c) ET in SRES, d) ET in RCP. The vertical dashed lines illustrate the climate periods used in SRES (1980–2010, 2011–2040, and 2041–2100). In RCPs, transient climate data were used (1980–2100) (For interpretation of the references to colour in this figure legend, the reader is referred to the web version of this article).

2013). From the impact viewpoint, one could thus argue that the characteristics of input uncertainty have not changed that much between these two generations of GCMs. Additional variability between RCP and SRES in our analysis was created by the fact that we did not have the same GCMs in the compiled subset of projections (see Suppl. A), and that the method for downscaling the results of GCMs for Finland differed between RCP and SRES. In SRES thirty-year periods of historical data were coupled with GCM projections to produce the climate for the whole century, while in the case of RCPs, the GCM projections directly provided the transient climate change from 1980 to 2100. This contributed to fairly different natural variability between RCP and SRES (Fig. 6, Suppl. A).

The dominant role of GCM over emission scenario as a driver of uncertainty of the impact studies outcome has not been pointed out in earlier Finnish studies (e.g. Kellomäki et al., 2008; Ge et al., 2013). In boreal-forest related studies this is of special importance due to the fact that the time perspective of tree growth approaches that of climate change. Our results demonstrate that impact studies with a single GCM projection may not expose the full range of possible changes and thus, may lack information about local/regional scale impacts that would be essential for decision making (e.g. Lung et al., 2013). Our understanding is that forest related climate mitigation policies do pose a risk that actions are based on mean response not on the range of scenarios, the relative probabilities of which cannot be specified at this point of time. It would therefore be extremely helpful for coherent decision-making if reporting overall uncertainty and its component sources was standard practise in scientific impact studies.

Structural uncertainty of the model, i.e., uncertainty due to our deficient scientific understanding of the process at hand, was represented here by the response of gas exchange to long-term CO_2 fertilization. Under the default assumptions, the direct influence of C_a on GPP (species pooled) was 50% of the total impact in A2 scenario and roughly 40% in A1B scenario and up to 38% in B1 at the end of the century, but the increase was sensitive to assumptions of C_a effects on WUE. Severe production limitations due to soil moisture availability seem unlikely if transpiration of trees is moderated by increased C_a. Without the assumptions of C_a-induced reductions of transpiration, there would be more sites suffering from drought in the future (Fig. 3b). Relative humidity (RH%) has been found to be a critical factor to differentiate the projected NPP among different Global Vegetation Models (Nishina et al., 2015). We derived vapor pressure deficit (D) using RH% predicted by the GCMs, while earlier Finnish studies have assumed unchanged RH% of air (e.g. Kellomäki et al., 2008; Ge et al., 2013), but both approaches lead to increased D. Earlier research concerning

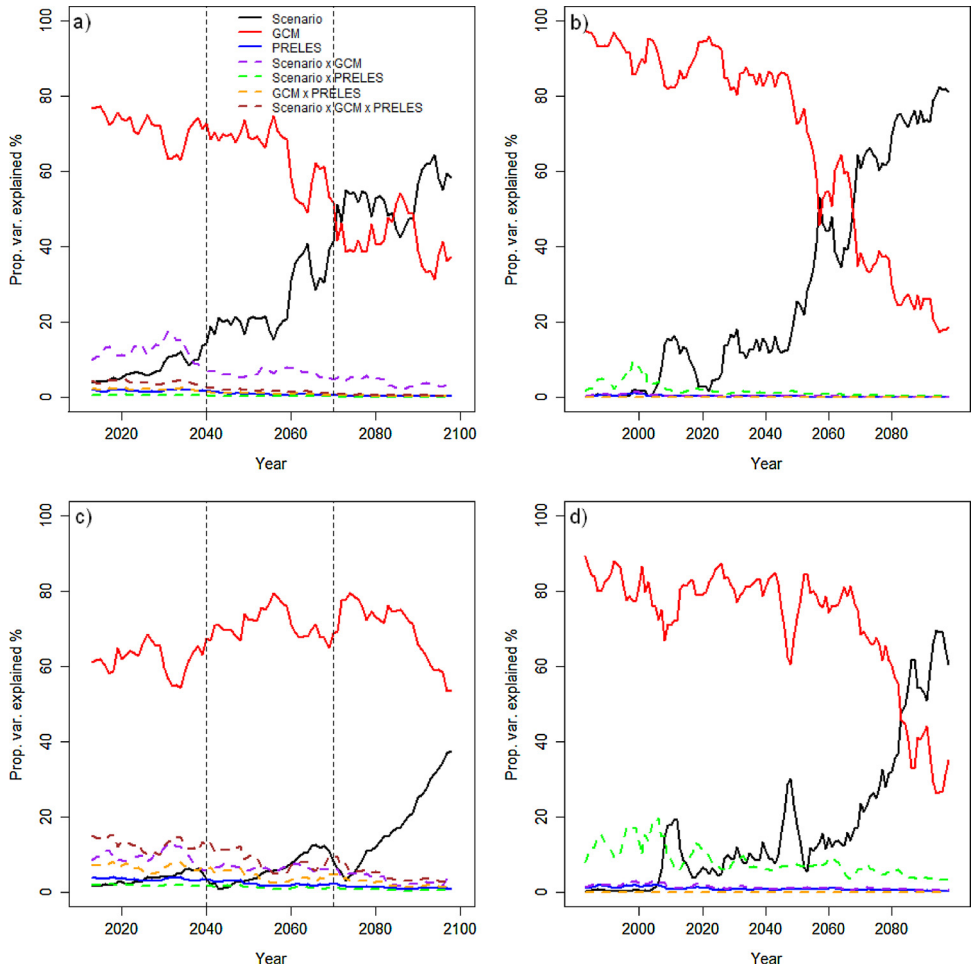

Fig. 6. ANOVA (see Eq. (11)) for Scots pine GPP and ET in one grid cell (Hyytiälä Forest Station) separately for RCP [RCP2.6, RCP4.5, RCP8.5], and SRES [A2, A1B, B1]). a) GPP in SRES b) GPP in RCP, c) ET in SRES and d) ET in RCP. The vertical dashed lines illustrate the climate periods used in SRES (1980–2010, 2011–2040, and 2041–2100). In RCPs, transient climate data were used (1980–2100).

Finland has warned about vulnerability to climate change of spruce growing on dry sites. However, based on our study, a crucial aspect for species management is that, species responsive to D and occupying moist sites will perform well. Drought-vulnerable sandy dry or uphill sites (Muukkonen et al., 2015) tend to be Scots-pine dominated already in the current climate. The species-specific responses of our study must be interpreted with caution, as the parameter adjustments were made subjectively on the basis of available but insufficient information. Concerning conclusions of these water effects, one has to keep in mind the weak ability of GCMs to represent within-year, seasonal and day-to-day variability of weather. This issue is the most critical one for rainfall since rains could become more sporadic and intense in the northern hemisphere (e.g. Jylhä et al., 2009; Rummukainen, 2012, 2013), with possibility off increased frequency of longer periods of drought. Neither we nor earlier studies accounted for this specific property of input uncertainty.

The applied PRELES model has been parameterized with several years of eddy-covariance data including considerable within-year variability of fluxes. We have found that the model also performs well at warmer and colder eddy-covariance sites (Minunno et al., 2016). Further support for plausible P predictions has been obtained through a comparison with the JSBACH model (Reick et al., 2013) at the scale of Finland (Peltoniemi et al., 2015). In this study, we found that the proportion of PRELES parametric uncertainty from total uncertainty was almost marginal in the projections of GPP. This indicates that lots of data were used in the calibration and the most important parameters were well constrained. We acknowledge that under the changing environmental conditions we were not able to fully separate model structural uncertainty from the parametric uncertainty but PRELES uncertainty here only describes the variability included in the calibration dataset (Minunno et al., 2016) and, thus, did not increase over time. This is a general challenge in calibration, especially in the case of simple models. It could be that processes not important in the current environment become major issues in the future, and thus the impact model uncertainty is not reflected coherently. One way forward could be to test PRELES with different CO_2 response functions against data from FACE experiments, and/or to calibrate the functions in such data sets. This could be very informative bearing in mind that the structural uncertainty related to this driver had a prominent effect on the model predictions. Our results also do not account for the possible increase in canopy size as a result of increasing GPP which could also lead to increasing ET and hence more pronounced drought effects, however, a comparison of simulations with different f_{aPPFD} values may provide a cue. In our simulations increasing f_{aPPFD} from 0.75 to 1 had an effect on E comparable to the (opposite) C_a-induced reduction of transpiration (Fig. SB2).

There are numerous effects we did not consider in our analysis. Restriction of tree response due to soil nitrogen limitation may down-regulate the CO_2 fertilization effect. Long-term growth stimulation has been found only under high nutrition (e.g. fertilized sites or on former agricultural land) or explained as a result of priming effects (see references in Palacio et al., 2014). The main effects of nutrients (particularly nitrogen as the main limiting nutrient in boreal forest) are (1) increased photosynthetic capacity of foliage (Reich et al., 1998;

Peltoniemi et al., 2012), and (2) increased carrying capacity, i.e., the total foliage that can be supported by the stand (Ladanai and Ågren, 2004; Mäkelä et al., 2008a,b). In boreal conifers the increased photosynthetic capacity due to variation in foliar N concentration is relatively modest (e.g. Peltoniemi et al., 2012), whereas the impacts of changes in carrying capacity could be considerable. The effects of increasing canopy cover and consequently f_{aPPFD} were already discussed above. However, whether or not the canopy cover will increase under climate change also depends on the response of nutrient availability to climate, as the increased CO_2 fertilisation is known to strengthen the carbon sink below ground under N limitation (Norby et al., 2010). Here, more information is needed on trends in N deposition, implications of the priming effect, as well as impacts of weather drivers on soil organic matter decomposition. In order to account for the nutrient cycle which could either up- or down-regulate the predicted increases in GPP, e.g. nitrogen modifier could be included in PRELES based on approaches like Peltoniemi et al. (2012). We also did not include any nitrogen deposition scenario. However, nitrogen deposition does not play a big role in Finland when compared with e.g. Central Europe. Also the effect of climate extremes and especially their connection to the changing disturbance regimes we did not include in the predictions. When considering the carbon cycling the increasing disturbances may have a much bigger role in the future than in current conditions (Seidl et al., 2017). All these additional effects will further increase the uncertainty of GPP projections into the future.

5. Conclusions

We consider it very likely that primary production of Finnish forests will be higher in the future than it is now. However, uncertainty around this mean response is very large and our decomposition of its sources demonstrates that more constraining information is needed equally on the biological mechanisms and on the expected environmental drivers before the projections can be made more conclusive. Regarding the mechanisms, we need to improve our scientific understanding of the interactions of CO_2 fertilization with water and nutrient fluxes (Figs. 2 and 3). At the same time, our analysis underlines the need of transparency in modelling studies about how input uncertainty from emission scenarios and different GCMs and their assumptions propagates to ecological impacts (Figs. 5 and 6). Transparency is easier to reach if the modelling approach is relatively simple, such as in the present study. It is encouraging in this respect that our results were much in line with previous studies obtained with highly mechanistic, complex models. We believe that these general methodological conclusions can be extended to more comprehensive models, such as models of the full vegetation carbon budget, although our example model only considered gross primary production.

Acknowledgements

We thank Pasi Kolari for the CO_2 modifier in PRELES model. We gratefully acknowledge the contribution of the Academy of Finland project CARB-ARC (No. 286190) and LIFE + financial instrument of the European Union (LIFE12 ENV/FI/000409 Monimet, http://monimet.fmi.fi).

The work was made in the frame of COST Action FP1304 PROFOUND.

Appendix A

List of the variables and functions of PRELES model.

Variable (model input or estimated by the model)	Symbol	Unit
Daily precipitation (water or snow)	R	mm
Drainage	F	mm
Drainage from surfacial water storage to soil (after $\theta_{surf,max}$ is reached)	F_{surf}	mm
Evapotranspiration from snow storage	E^{snow}	mm
Evapotranspiration from soil storage	E^{soil}	mm
Evapotranspiration from surficial water storage	E^{surf}	mm
Fraction of absorbed photosynthetic photon flux density	f_{aPPFD}	–
Gross primary production	P	g Cm^{-2}
Leaf area index	L_A	–
Light modifier	f_L	–
Minimum of vapour pressure deficit and soil water modifier	$f_{DW,P}$	–
Modifier for temperature acclimation state, cf. S	f_S	–
Photosynthetic photon flux density	Φ	mol^{-1}
Rainfall, as rain	R^1	mm
Relative extractable water	W	–
Soil water modifier for evaporation	$f_{W,E}$	–
Snow/ice water content (in water equivalents)	θ_{snow}	mm
Snowfall	R°	mm
Snowmelt	M	mm
Soil water content	θ	mm
Soil water modifier for gross primary production	$f_{W,P}$	–
State of acclimation to temperature	S	°C
Surfacial water content, e.g. on leaf and soil surfaces (has an upper limit defined by subscript max')	θ_{surf}	mm
Temperature, daily mean	T	°C
Vapour pressure deficit, daily mean	D	kPA
Vapour pressure deficit modifier	f_D	–

Appendix B. Supplementary data

Supplementary material related to this article can be found, in the online version, at doi:https://doi.org/10.1016/j.agrformet.2018.06.030.

References

Aalto, J., Pirinen, P., Heikkinen, J., Venäläinen, A., 2013. Spatial interpolation of monthly climate data for Finland: comparing the performance of kriging and generalized additive models. Theor. Appl. Climatol. 112, 99–111.

Ahlström, A., Schurgers, G., Arnet, A., Smith, B., 2012. Robustness and uncertainty in terrestrial ecosystem carbon response to CMIP5 climate change projections. Environ. Res. Lett. 7, 1–9.

Ainsworth, E.A., Rogers, A., 2007. The response of photosynthesis and stomatal conductance to rising [CO2]: mechanisms and environmental interactions. Plant Cell Environ. 30, 258–270.

Allen, C.D., Macalady, A.K., Chenchouni, H., Bachelet, D., McDowell, N., Vennetier, M., Kitzberger, T., Rigling, A., Breshears, D.D., Hogg, E.H.T., Gonzalez, P., Fensham, R., Zhang, Z., Castro, J., Demidova, N., Lim, J.-H., Allard, G., Running, S.W., Semerci, A., Cobb, N., 2010. A global overview of drought and heat-induced tree mortality reveals emerging climate change risks for forests. For. Ecol. Manage. 259, 660–684.

Bergh, J., Freeman, M., Sigurdsson, B., Kellomäki, S., Laitinen, K., Niinistö, S., Peltola, H., Linder, S., 2003. Modelling the short-term effects of climate change on the productivity of selected tree species in Nordic countries. For. Ecol. Manage. 183, 327–340.

Bonan, G.B., 2008. Forests and climate change: forcings, feedbacks, and the climate benefits of forests. Science 320, 1444–1449.

Bright, R.M., Antón-Fernández, C., Astrup, R., Cherubini, F., Kvalevåg, M., Strømman, A.H., 2014. Climate change implications of shifting forest management strategy in a boreal forest ecosystem of Norway. Global Change Biol. 20, 607–621.

Cavanagh, Rachel D., Murphy, Eugene J., Bracegirdle, Thomas J., Turner, John, Knowland, Cheryl A., Corney, Stuart P., Smith Jr., Walker O., Waluda, Claire M., Johnston, Nadine M., Bellerby, Richard G.J., Constable, Andrew J., Costa, Daniel P., Hofmann, Eileen E., Jackson, Jennifer A., Staniland, Iain J., Wolf-Gladrow, Dieter, Xavier, JoséC., 2017. A synergistic approach for evaluating climate model output for ecological applications. Front. Mar. Sci. 4.

Dewar, R.C., Medlyn, B.E., McMurtrie, R.E., 1998. A mechanistic analysis of light and carbon use efficiencies. Plant Cell Environ. 21, 573–588.

Ellsworth, D.S., Reich, P.B., Naumburg, S.E., Koch, G.W., Kubiske, M.E., Smith, S.D., 2004. Photosynthesis, carboxylation and leaf nitrogen responses of 16 species to elevated pCO2 across four free-air CO2 enrichment experiments in forest, grassland and desert. Glob. Change Biol. 10, 2121–2138.

Farquhar, G.D., Caemmerer, S., Berry, J., 1980. A biochemical model of photosynthetic CO_2 assimilation in leaves of C3 species. Planta 149, 78–90.

Forzieri, G., Alkama, R., Miralles, D.G., Cescatti, A., 2017. Satellites reveal contrasting responses of regional climate to the widespread greening of earth. Science 356, 1180–1184.

Ge, Z., Kellomäki, S., Peltola, H., Zhou, X., Väisänen, H., Strandman, H., 2013. Impacts of climate change on primary production and carbon sequestration of boreal Norway spruce forests: Finland as a model. Clim. Change 118, 259–273.

Horemans, J.A., Bosela, M., Dobor, L., Barna, M., Bahyl, J., Deckmyn, G., Fabrika, M., Sedmak, R., Ceulemans, R., 2016. Variance decomposition of predictions of stem biomass increment for European beech: contribution of selected sources of uncertainty. For. Ecol. Manage. 361, 46–55.

IPCC, 2007. Climate change 2007: the physical science basis. Contribution of Working Group I to the Fourth Assessment Report of the Intergovernmental Panel on Climate Change. Cambridge University Press, Cambridge, United Kingdom and New York, NY, USA.

IPCC, 2013. Climate change 2013: the physical science basis. In: Stocker, T.F., Qin, D., Plattner, G.-K., Tignor, M., Allen, S.K., Boschung, J., Nauels, A., Xia, Y., Bex, V., Midgley, P.M. (Eds.), Contribution of Working Group I to the Fifth Assessment Report of the Intergovernmental Panel on Climate Change. Cambridge University Press, Cambridge, United Kingdom and New York, NY, USA, pp. 1535. https://doi.org/10.1017/CBO9781107415324.

Jylhä, K., Ruosteenoja, K., Räisänen, J., Venäläinen, A., Tuomenvirta, H., Ruokolainen, L., Saku, S., Seitola, T., 2009. The changing climate in Finland: estimates for adaptation studies. ACCLIM Project Report 2009. Finn Meteorol Inst. Reports 4.

Keenan, T.F., Hollinger, D.Y., Bohrer, G., Dragoni, D., Munger, J.W., Schmid, H.P., Richardson, A.D., 2013. Increase in forest water-use efficiency as atmospheric carbon dioxide concentrations rise. Nature 499, 324–327.

Kellomäki, S., Peltola, H., Nuutinen, T., Korhonen, K.T., Strandman, H., 2008. Sensitivity of managed boreal forests in Finland to climate change, with implications for adaptive management. Philos. Trans. R. Soc. B: Biol. Sci. 363, 2339–2349.

Knutti, R., Masson, D., Gettelman, A., 2013. Climate model genealogy: generation CMIP5 and how we got there. Geophys. Res. Lett. 40, 1194–1199.

Kolari, P., Kulmala, L., Pumpanen, J., Launiainen, S., Ilvesniemi, H., Hari, P., Nikinmaa, E., 2009. CO_2 exchange and component CO_2 fluxes of a boreal Scots pine forest. Bor. Environ. Res. 14, 761–783.

Ladanai, S., Ågren, G.I., 2004. Temperature sensitivity of nitrogen productivity for Scots pine and Norway spruce. Trees 18, 312–319.

Lehtonen, I., Venäläinen, A., Kämäräinen, M., Peltola, H., Gregow, H., 2016. Risk of large-scale fires in boreal forests of Finland under changing climate. Nat. Hazards Earth Syst. Sci. 16, 239–253.

Leuning, R., 1995. A critical appraisal of a combined stomatal-photosynthesis model for C3 plants. Plant Cell Environ. 18, 339–355.

Linkosalo, T., Lappalainen, H.K., Hari, P., 2008. A comparison of phenological models of leaf bud burst and flowering of boreal trees using independent observations. Tree Physiol. 28, 1873–1882.

Liski, J., Lehtonen, A., Palosuo, T., Peltoniemi, M., Eggers, T., Muukkonen, P., Mäkipää, R., 2006. Carbon accumulation in Finland's forests 1922–2004 – and estimate obtained by combination of forest inventory data with modelling of biomass, litter and soil. Ann. Sci. 63, 687–697.

Lung, T., Dosio, A., Becker, W., Lavalle, C., Bouwer, L.M., 2013. Assessing the influence of climate model uncertainty on EU-wide climate change impact indicators. Clim. Change 120, 211–227.

Ma, J., Yan, X., Dong, W., Chou, J., 2015. Gross primary production of global forest ecosystems has been overestimated. Nat. Sci. Rep. 5, 1–9.

Mäkelä, A., Valentine, H.T., 2001. The ratio of NPP to GPP: evidence of change over the course of stand development. Tree Phys. 21, 1015–1030.

Mäkelä, A., Kolari, P., Karimäki, J., Nikinmaa, E., Perämäki, M., Hari, P., 2006. Modelling five years of weather-driven variation of GPP in a boreal forest. Agric. For. Meteorol. 139, 382–398.

Mäkelä, A., Pulkkinen, M., Kolari, P., Lagergren, F., Berbigier, P., Lindroth, A., Loustau, D., Nikinmaa, E., Vesala, T., Hari, P., 2008a. Developing an empirical model of stand GPP with the LUE approach: analysis of eddy covariance data at five contrasting conifer sites in Europe. Glob. Change Biol. 14, 92–108.

Mäkelä, A., Valentine, H.T., Helmisaari, H.-S., 2008b. Optimal co-allocation of carbon and nitrogen in a forest stand at steady state. N. Phytol. 180, 114–123.

Mäkelä, A., Pulkkinen, M., Mäkinen, H., 2016. Bridging empirical and carbon-balance based forest site productivity – significance of below-ground allocation. For. Ecol. Manage. 372, 64–77.

Medlyn, B.E., Duursma, R.A., Zeppel, M.J.B., 2011. Forest productivity under climate change: a checklist for evaluating model studies. Wiley Interdiscip. Rev. Clim. Change 2, 332–355.

Meehl, G.A., Covey, C., Delworth, T., Latif, M., McAvaney, B., Mitchell, J.F.B., Stouffer, R.J., Taylor, K.E., 2007. The WCRP CMIP3 multimodel dataset: a new era in climate change research. Bull. Am. Meteorol. Soc. 88, 1383–1394.

Minunno, F., Peltoniemi, M., Launiainen, S., Aurela, M., Lindroth, A., Lohila, A., Mammarella, I., Minkkinen, K., Mäkelä, A., 2016. Calibration and validation of a semi-empirical flux ecosystem model for coniferous forests in the oreal region. Ecol. Model. 341, 37–52.

Moss, R.H., Edmonds, J.A., Hibbard, K.A., Manning, M.R., Rose, S.K., Vuuren, D.P., van, Carter, T.R., Emori, S., Kainuma, M., Kram, T., Meehl, G.A., Mitchell, J.F.B., Nakicenovic, N., Riahi, K., Smith, S.J., Stouffer, R.J., Thomson, A.M., Weyant, J.P., Wilbanks, T.J., 2010. The next generation of scenarios for climate change research and assessment. Nature 463, 747–756.

Muukkonen, P., Nevalainen, S., Lindgren, M., Peltoniemi, M., 2015. Spatial occurrence of drought associated damage in Finnish boreal forests: results from forest condition monitoring and GIS analysis. Bor. Environ. Res. 20, 172–180.

Nishina, K., Ito, A., Falloon, P., Friend, A.D., Beerling, D.J., Ciais, P., Clark, D.B., Kahana, R., Kato, E., Lucht, W., Lomas, M., Pavlick, R., Schaphoff, S., Warsawaski, L., Yokohata, T., 2015. Decomposing uncertainties in the future terrestrial carbon budget associated with emission scenarios, climate projections, and ecosystem simulations using the ISI-MIP results. Earth Syst. Dynam. 6, 435–445.

Norby, R.J., Warren, J.M., Iversen, C.M., Medlyn, B.E., McMurtrie, R.E., 2010. CO2 enhancement of forest productivity constrained by limited nitrogen availability. PNAS 107 (45), 19368–19373.

Norby, R.J., Zak, D.R., 2011. Ecological lessons from free-air CO2 enrichment (FACE) experiments. Ann. Rev. Ecol. Evol. Syst. 42, 181–203.

Novick, K.A., Oishi, A.C., Ward, E.J., Siqueira, M.B.S., Juang, J.-Y., Stoy, P.C., 2015. On the difference in the net ecosystem exchange of CO2 between deciduous and evergreen forests in the southeastern United States. Glob. Change Biol. 21, 827–842.

Ollikainen, M., 2014. Forestry in bioeconomy – smart green growth for the humankind. Scand. J. Respir. Dis. 29, 360–366.

Ollinger, S.V., Goodale, C.L., Hayhoe, K., Jenkins, J.P., 2007. Potential effects of climate change and rising CO2 on ecosystem processes in northeastern U.S. forests. Mitig. Adapt. Strateg. Glob. Change 13, 476–485.

Palacio, S., Hoch, G., Sala, A., Körner, C., Millard, P., 2014. Does carbon storage limit tree growth? N. Phytol. 201, 1096–1100.

Peltola, H., Ikonen, V.P., Gregow, H., Strandman, H., Kilpeläinen, A., Venäläinen, A., Kellomäki, S., 2010. Impacts of climate change on timber production and regional risks of wind-induced damage to forests in Finland. For. Ecol. Manage. 260, 833–845.

Peltoniemi, M., Pulkkinen, M., Kolari, P., Duursma, R.A., Montagni, L., Wharton, S., Lagergren, F., Takagi, K., Verbeeck, H., Christensen, T., Vesala, T., Falk, M., Loustau, D., Mäkelä, A., 2012. Does canopy mean nitrogen concentration explain variation in canopy light use efficiency across 14 contrasting forest sites. Tree Phys. 32, 200–218.

Peltoniemi, M., Pulkkinen, M., Aurela, M., Pumpanen, J., Kolari, P., Mäkelä, A., 2015. A semi-empirical model of boreal forest gross primary production, evapotranspiration, and soil water – calibration and sensitivity analysis. Bor. Environ. Res. 20, 151–171.

Reich, P.B., Ellsworth, D.S., Walters, M.B., 1998. Leaf structure (specific leaf area) modulates photosynthesis-nitrogen relations: evidence from within and across species and functional groups. Funct. Ecol. 12, 948–958.

Reich, P.B., Rich, R.I., Lu, X., Wang, Y.-P., Oleksyn, J., 2014. Biogeographic variation in evergreen conifer needle longevity and impacts on boreal forest carbon cycle projections. Proc. Natl. Acad. Sci. U. S. A. 111, 13703–13708.
Reick, C.H., Raddatz, T., Brovkin, V., Gayler, V., 2013. Representation of natural and anthropogenic land cover change in MPI-ESM. J. Adv. Model. Earth Syst. 5, 459–482.
Reyer, C., Lasch-Born, P., Suckow, F., Gutsch, M., Murawski, A., Pilz, T., 2014. Projections of regional changes in forest net primary productivity for different tree species in Europe driven by climate change and carbon dioxide. Ann. Sci. 71, 211–225.
Rötter, R.P., Höhn, J., Trnka, M., Fronzek, S., Carter, T.R., Kahiluoto, H., 2013. Modelling shifts in agroclimate and crop cultivar response under climate change. Ecol. Evol. 3, 4197–4214.
Rummukainen, M., 2012. Changes in climate and weather extremes in the 21st century. WIREs Clim. Change 3, 115–129.
Rummukainen, M., 2013. Climate change: changing means and changing extremes. Clim. Change 121, 3–13.
Ruosteenoja, K., Räisänen, J., Pirinen, P., 2011. Projected changes in thermal seasons and the growing season in Finland. Int. J. Climatol. 31, 1437–1487.
Ruosteenoja, K., Jylhä, K., Kämäräinen, M., 2016. Climate projections for Finland under the RCP forcing scenarios. Geophysica 51, 17–50.
Seidl, R., Thom, D., Kautz, M., Martin-Benito, D., Peltoniemi, M., Vacchiano, G., Wild, J., Ascoli, D., Petr, M., Honkaniemi, J., Lexer, M.J., Trotsiuk, V., Mairota, P., Svoboda, M., Fabrika, M., Nagel, T.A., Reyer, C.P.O., 2017. Forest disturbances under climate change. Nat. Clim. Change 395–402.
Sievänen, R., Salminen, O., Lehtonen, A., Ojanen, P., Liski, J., Ruosteenoja, K., Tuomi, M., 2014. Carbon stock changes of forest land in Finland under different levels of wood use and climate change. Ann. Sci. 71, 255–265.
Snyder, P.K., Liess, S., 2014. The simulated atmospheric response to expansion of the Arctic boreal forest biome. Clim. Dyn. 42, 487–503.
Snyder, P.K., Delire, C., Foley, J.A., 2004. Evaluating the influence of different vegetation biomes on the global climate. Clim. Dyn. 23, 279–302.
Storn, R., Price, K., 1997. Differential evolution— a simple and efficient heuristic for global optimization over continuous spaces. J. Glob. Optim. 11, 341–359.
ter Braak, C.J.F., 2006. A Markov chain Monte Carlo version of the genetic algorithm differential evolution: easy Bayesian computing for real parameter spaces. Stat. Comput. 16, 239–249.
ter Braak, C.J., Vrugt, J.A., 2008. Differential evolution Markov chain with snooker updater and fewer chains. Stat. Comput. 18, 435–446.
Unger, N., 2014. Human land-use-driven reduction of forest volatiles cools global climate. Nat. Clim. Change 4, 907–910. https://doi.org/10.1038/NCLIMATE2347.
Uusitalo, L., Lehikoinen, A., Helle, I., Myrberg, K., 2015. An overview of methods to evaluate uncertainty of deterministic models in decision support. Environ. Modell. Softw. 63, 24–31.
van Oijen, M., Reyer, C., Bohn, F.J., Cameron, D.R., Deckmyn, G., Felchsig, M., Härkönen, S., Hartig, F., Huth, A., Kiviste, A., Lasch, P., Mäkelä, A., Mette, T., Minunno, F., Rammer, W., 2013. Bayesian calibration, comparison and averaging of six forest models, using data from Scots pine stands across Europe. For. Ecol. Manage. 289, 255–268.
van Vuuren, D.P., Carter, T.R., 2014. Climate and socio-economic scenarios for climate change research and assessment: reconciling the new with the old. Clim. Change 122, 415–429.
van Vuuren, D.P., Edmonds, J., Kainuma, M., Riahi, K., Thomson, A., Hibbard, K., Hurtt, G.C., Kram, T., Krey, V., Lamarque, J.-F., Masui, T., Meinshausen, M., Nakicenovic, N., Smith, S.J., Rose, S.K., 2011. The representative concentration pathways: an overview. Clim. Change 109, 5–31.
Veijalainen, N., Lotsari, E., Alho, P., Vehviläinen, B., Käyhkö, J., 2010. National scale assessment of climate change impacts on flooding in Finland. J. Hydrol. 391, 333–350.
Venäläinen, A., Tuomenvirta, H., Pirinen, P., Drebs, A., 2005. A basic Finnish climate data set 1961–2000-description and illustration. Finn. Meteorol. Inst. Rep. 5.
Wagle, P., Xiao, X., Kolb, T.E., Law, B.E., Wharton, S., Monson, R.K., Chen, J., Blanken, P.D., Novick, K.A., Dore, S., Noormets, A., Gowda, P.H., 2016. Differential responses of carbon and water vapor fluxes to climate among evergreen needleleaf forests in the USA. Ecol. Process. 5, 8.
Wamelink, G.W.W., Wieggers, H.J.J., Reinds, G.J., Kros, J., Mol-Dijkstra, J.P., van Oijen, M., de Vries, W., 2009. Modelling impacts of changes in carbon dioxide concentration, climate and nitrogen deposition on carbon sequestration by European forests and forest soils. For. Ecol. Manage. 258, 1794–1805.
Waring, R.H., Landsberg, J.J., Williams, M., 1998. Net primary production of forests: a constant fraction of gross primary production? Tree Phys. 18, 129–134.